RSC Advances

ROYAL SOCIETY OF CHEMISTRY

www.rsc.org/advances

Cite this: DOI: 10.1039/c0xx00000x

www.rsc.org/xxxxxx

PAPER

Electron induced chemistry of disilane

Dhanoj Gupta, Rahla Naghma, Biplab Goswami and Bobby Antony*

Received (in XXX, XXX) Xth XXXXXXXXX 20XX, Accepted Xth XXXXXXXXX 20XX

DOI: 10.1039/b000000x

Theoretical study of electron impact scattering by disilane molecule is reported in this article. Total, elastic, excitation and differential cross sections were computed at low incident energies using R-matrix method through QUANTEMOL-N. The total cross section calculation was extended to higher energies using spherical complex optical potential formalism. The smooth transition at the overlap of two formalisms around the ionization threshold of the target has helped to predict cross sections over a wide energy range from 0.1 eV to 5 keV. The resonance position predicted by the present static exchange and static exchange plus polarization models at 3.3 and 3.0 eV respectively agrees quite well with previous theoretical and experimental results. The inclusion of polarization effects in the calculation has considerably improved the position of the resonance from the previous static exchange calculation. In general the results obtained for total, elastic and differential cross sections show reasonable agreement with the experiment. The excitation cross section of disilane from ground state to various excited states is reported for the first time.

1. Introduction

Silicon is an important element used for many applications in semiconductor industry. Various optoelectronic devices, such as thin film solar cells, thin film transistors and numerous other switching devices uses nanocrystalline silicon and polycrystalline silicon films [1,2]. The demand and use of collision cross section data for polyatomic molecules at low energy regime by electron impact have grown considerably due to their application in cold plasmas in the processing and fabrication of materials [3]. The importance of cross section data for e-Si_2H_6 system in the semiconductor technology [4,5] has stimulated the interest for this calculation. An extensive range of accurate collision cross section data for e-Si_2H_6 system is required for modeling and diagnostic of disilane containing low temperature plasmas having possible application in the processing and fabrication of microelectronic materials and devices [6]. Although, the low energy cross section data for polyatomic molecules play an important role in modeling industrial and atmospheric plasmas, there is still dearth in experimental [7] and theoretical [8] cross sections for these systems.

Despite the importance and application of this molecule to diverse areas of sciences, only limited attention has been given to e-Si_2H_6 scattering system at low energy regime. Winstead *et al* [8] have computed elastic electron scattering cross sections viz. integral, differential and momentum transfer cross sections for Si_2H_6 from 5 to 30 eV using an implementation of the Schwinger multichannel method (SMC) using distributed memory parallel computer architecture (SMC-ae). SMC-ae is the parallel computer code in which all electrons are taken into account. The results were obtained within the static exchange (SE) approximation. Bettega *et al* [9] made use of the SMC method implemented with the local-density norm-conserving pseudo-potentials (SMC-pp) for the calculation of integral elastic and differential elastic cross sections for the targets CH_4, SiH_4, GeH_4 and Si_2H_6. In SMC-pp version the core electrons are substituted by the pseudo-potentials and only the valence electrons are taken into consideration and described explicitly. The results are obtained within the SE approximation and are compared with the previous SMC-ae results of Winstead *et al* [8]. Later Bettega *et al* [10,11] used SMC method for the calculation of integral and differential cross sections for elastic scattering of electrons by X_2H_6 (X= B, C, Si, Ge) and methylsilane. The calculations were performed within SE approximation. The results for methylsilane were compared with C_2H_6 and Si_2H_6. The integral and differential cross sections for Si_2H_6 were compared with the available experimental results of Dillon *et al* [12] as well.

Dillon *et al* [12] have measured the elastic differential cross sections (DCS) for e-disilane system for the incident energy from 2 to 100 eV at an angular range of 10-130^0. The DCS have been integrated by employing a nonlinear phase shift fitting procedure to obtain the integral elastic and momentum transfer cross sections. The continuum multiple scattering (CMS) calculations were also performed by Dillon *et al* [12] for comparing their measurements. The agreement between the measurement and calculation was found to be good. But, their elastic cross section shows a broad peak at around 5 eV which does not agree with any of the previously available results in terms of position and magnitude. Their inelastic energy loss spectrum shows a sharp peak at around 2 eV, which they attribute to a shape resonance by

the trapping of electron temporarily in a Si-H anti-bonding molecular orbital. They have also recorded the electron energy loss spectra of disilane over excitation energy of 20 eV and have given the excitation energy of disilane for various triplet and singlet states [13]. The lone measurement of the absolute total cross section (TCS) for e-disilane system is done by Szmytkowski *et al* [6] in the energy range from 1 to 370 eV in a linear transmission experiment. There are very few experimental and theoretical works carried out for this target. At low energy regime there is a serious disagreement between the experiments of Dillon *et al* [12] and Szmytkowski *et al* [6]. The SMC and CMS calculations of Bettega *et al* [9-11] and Dillon *et al* [12] for elastic cross sections at low energies shows deviation from each other and the position of resonance and magnitude of cross section does not give a good agreement. In the intermediate energy range, Vinodkumar *et al* [14] have computed the total cross section for disilane from ionization threshold to 5000 eV using spherical complex optical potential (SCOP) formalism. Their cross section agrees quite well with the measurement of Szmytkowski *et al* [6] above 30 eV, below which it overestimates the experimental values.

So the investigations on disilane using electron as probe are fragmentary and the reported results are limited to either low or high energy. This has motivated to study this molecule and produce reliable cross section data for a wide energy range (0.1 – 5000 eV). At low energy regime the polarization effects are also included in the SE calculation to get improved results. In the present study, we have used two distinct formalisms: R-matrix [15] below the ionization threshold and SCOP [16-19] beyond that till 5000 eV. The extension of the low energy calculation to higher energies is possible due to a good matching of cross sections at the overlapping energy. The excitation cross sections from ground state to different excited states are also computed for which there is no comparison available to the best of our knowledge.

2. Theoretical Methodology

The theoretical methods employed here comprise of two distinct formalisms namely R-matrix for low energy up to 10 eV and the SCOP formalism from ionization threshold to 5 keV. The two methodologies are known to work very efficiently at their respective energy range [17]. For the low energy calculation, the representation of the target model employed for the calculation is very important as it ensures accurate and reliable results. Section 2.1 describes the target model used for present calculation and the target parameters obtained in the calculation. In sections 2.2 and 2.3 the R-matrix and SCOP methods are described explicitly.

2.1. Target model used for low energy calculations

Disilane (Si_2H_6) has two trigonal pyramidal silicon atoms with hydrogen atoms attached to it with Si-H bond length of 1.47 Å [20]. The silicon atoms bond linearly with Si-Si bond length of 2.32 Å [20]. All calculations in this work are carried out at the equilibrium geometry of the target using C_s point group symmetry which is the sub-group of D_{3d} point group (the natural point group symmetry of Si_2H_6). The double zeta plus polarisation (DZP) basis set is employed for the construction of the target wave functions. The ground state Hartree-Fock electronic configuration is represented as $1a'^2$, $2a'^2$, $3a'^2$, $4a'^2$, $5a'^2$, $6a'^2$, $1a''^2$, $7a'^2$, $2a''^2$, $8a'^2$, $9a'^2$, $10a'^2$, $11a'^2$, $3a''^2$, $12a'^2$, $4a''^2$, $13a'^2$. Out of 34 target electrons 20 electrons are frozen in 1a', 2a', 3a', 4a', 5a', 6a', 7a', 8a', 1a", 2a" molecular orbitals and the remaining 14 electrons are kept in the active space of 9a', 10a', 11a', 12a', 13a', 14a', 15a', 3a", 4a", 5a" molecular orbitals. A total number of 2528 configuration state functions (CSFs) are generated for the representation of seven target states for the ground state and 95 channels are included in the calculation.

The target properties reflect the goodness of the target model employed. In the present study, we have obtained the ground state energy of -581.669 hartree which matches exactly with the theoretical value of -581.669 hartree given in the Computational Chemistry Comparison and Benchmark Database (CCCBDB) [20]. The present rotational constant 1.45 cm^{-1} agrees well with the experimental value 1.43 cm^{-1} [20]. For the molecules belonging to the D_{3d} point group symmetry, there is no dipole moment which is very much evident from the present calculation giving the dipole moment to be zero. The first electronic excitation energy obtained in the present calculation is 7.74 eV which is slightly higher than the experimental value of 6.3 eV reported by Dillon *et al* [13]. This discrepancy in the excitation energy may be due to the use of reduced point group symmetry C_s in our calculation instead of its natural point group D_{3d}. The target properties along with the available comparisons are summarized in table 1.

Table 1. Target properties obtained for the e-Si_2H_6 molecule.

Properties of Si_2H_6	Present	Experimental	Theoretical
Ground-state energy (au)	-581.323	-	-581.669 [20]
First excitation energy (eV)	7.74	6.3 [13]	-
Rotational constant (cm^{-1})	1.45	1.43 [20]	-
Dipole moment(D)	0.0	-	-

2.2. Low energy formalism (1 eV to ~ 15 eV)

The *ab-initio* methods such as R-matrix method [15], Schwinger multichannel method [21] and Kohn variational method [22] are used for the calculations of various reliable cross sections viz., elastic, inelastic, differential, momentum transfer etc at low energy regime, which is a significant advancement in the field of electron-molecule collision. In the *ab-initio* methods, there are basically two important levels of approximations used for the calculations such as static exchange (SE) and static exchange plus polarization (SEP). Out of the two SE is the simplest of approximation used for the calculation of cross section. SEP model includes the polarization effects in the calculation, which improves the quality of results. In recent past, Altunata *et al* [23] have introduced an *ab-initio* R-matrix method using an iterative

Green's-function for determining the molecular reaction matrix of scattering theory with smooth energy dependence. This method mostly takes care of all the polarization effects and treats both polar and non polar ion cores in a unified fashion and is equally valid for both short and long range potentials. They have calculated the Rydberg and Continuum electronic states of calcium monofluoride (CaF), which has a highly polar ion core [24]. The *ab-initio* calculations depend mostly on the evaluation of accurate and reliable molecular integrals or matrix elements. Wong *et al* [25] have given closed-form analytic expressions for one- and two-electron integrals of Cartesian Gaussian orbitals outside the R-matrix sphere which can be used in *ab-initio* molecular scattering calculations. The molecular integral expressions for multielectron R-matrix methods are also presented in a closed form in their approach. It is a known fact that R-matrix method is the most widely used *ab-initio* methods. In this method the configuration space is divided into an inner region and an outer region. The inner region is a sphere of radius of about 10 a.u., while the outer region is infinite. For the present calculation, the outer region is chosen to be a sphere of radius 100 a.u. In the inner region, the scattering electron and target electrons are indistinguishable, which makes the inner region problem complex with all the interaction potentials namely static, exchange and correlation polarization potentials embedded in it. The radius of the inner region is chosen in such a way that it incorporates the total wave function of the target states included in the calculation. For the solution of the inner region, standard quantum chemistry codes are employed which gives precise and accurate solution taking the maximum time of the calculation. Moreover, the inner region problem is independent of the energy of the scattering electron and is required to be solved only once. In the outer region, the problem becomes simpler as the scattering electron is quite far from the centre of mass of the target and only the long range multipolar interactions is dominant in this region. Here, single centre close-coupling approximation is used which takes less time for calculation and the solution is obtained quickly. The problem in the outer region is dependent on the energy of the scattering electron. The calculations performed in the present study assume a fixed nuclei approximation at the equilibrium geometry of the molecule.

The time independent Schrödinger equation is solved using the inner region wave function constructed through close coupling approximation [26] given by,

$$\psi_k^{N+1} = A\sum_I \psi_I^N(x_1,\cdots,x_N)\sum_j \zeta_j(x_{N+1})a_{Ijk} + \sum_m \chi_m(x_1,\cdots,x_{N+1})b_{mk} \quad (1)$$

Here A is the anti-symmetrization operator obtained by imposing Pauli's exclusion principle on the electrons. ψ_I^N is the wavefunction of target and x_N are the spatial and spin coordinates of the nth target electron, ζ_j are continuum orbital spin-coupled with the scattering electron and a_{ijk} and b_{mk} are variational coefficients determined by the diagonalization of Hamiltonian matrix. The first summation runs over the configuration used in the close-coupling approximation and second summation over the continuum orbitals. Hence, the first term represents target plus continuum orbitals in the calculations where a static exchange calculation has a single Hartree-Fock target state. The second term runs over configurations χ_m, where all electrons are placed in target molecular orbitals. The present calculation uses the lowest number of target states, represented by a configuration interaction (CI) expansion in the first expansion and over thousands of configurations in the second. In the present case, 7 lowest energetically excited target states are used. These configurations allow for both orthogonality relaxation and short-range polarization effects. The Hartree-Fock Self-Consistent Field method with Gaussian-type orbitals and the continuum orbitals of Faure *et al.* [27] are used for the representation of complete molecular orbitals in terms of occupied and virtual target molecular orbitals and included up to g (l = 4) orbitals. The partial wave expansion is used to solve Schrödinger equation for the electron-molecule interacting system due to its high efficiency at low energy regime and rapid convergence. The R-matrix acts as bridge between the inner region and the outer region boundary. The solution of the inner region is propagated to the outer region where it is matched with the asymptotic functions given by Gailitis expansion [28]. In the outer region, the coupled single centre equations describing the scattering are integrated to get the K-matrix elements. The diagonalization of the K-matrix gives the eigenphase sum, which is used to obtain the position and width of the resonances, if any. The K-matrices are used to obtain the T-matrices as follows,

$$T = \frac{2iK}{1 - iK} \quad (2)$$

The T-matrices are in turn used to calculate various cross sections. The differential cross section (DCS) can also be evaluated employing K-matrices using the POLYDCS program of Sanna and Gianturco [29].

2.3. High energy formalism

The intermediate to high energy calculations were carried out using the SCOP formalism. The formulation of the interaction potential representing the electron target scattering system is given by the complex optical potential as,

$$V_{opt}(r,E_i) = V_R(r) + iV_I(r,E_i) \quad (3)$$

The real part of the total potential of the system given in equation (3) consists of static, exchange and polarization potentials as,

$$V_R(r,E_i) = V_{st}(r) + V_{ex}(r,E_i) + V_p(r,E_i) \quad (4)$$

These potentials are the functions of incident energy (E_i) and radial distance (r) and accounts for various electron target interaction during collision. The basic input required for the formulation of these potential are the charge density of the target, $\rho(r)$, ionization potential and electric dipole polarizability. The charge density of the target molecule is derived from the atomic charge densities of the atom using the parameterized Hartree-Fock wave function of Salvat *et al* [30]. For the present e-Si_2H_6, we have used a single centre approach by expanding the charge density of the Si atom from the centre of mass of the Si_2 and the lighter hydrogen atoms are expanded from the centre of the mass of the system by using the Bessel function expansion method given by Gradashteyn and Ryzhik [31]. For the static potential (V_{st}) we have used the H-F parameters given by Salvat *et al* [30], for the exchange potential (V_{ex}) the parameter free Hara's free electron model [32] is used and for the polarization potential (V_p), the correlation potential of Zhang *et al.* [33] is employed. The

imaginary part of the potential given in equation (3) corresponds to the loss of incident flux to the absorption or inelastic channel, which is developed from the model potential of Staszewska *et al.* [34] given by,

$$V_{abs}(r,E_i) = -\rho(r)\sqrt{\frac{T_{loc}}{2}}\left(\frac{8\pi}{10k_F^3E_i}\right)\theta(p^2-k_F^2-2\Delta)(A_1+A_2+A_3) \quad (5)$$

Where the local kinetic energy is given by,

$$T_{loc} = E_i - (V_{st}+V_{ex}+V_p) \quad (6)$$

Here, $p^2 = 2E_i$ and $k_F = \left[3\pi^2\rho(r)\right]^{1/3}$ is the Fermi wave vector. The functions A_1, A_2 and A_3 depend differently on the Heaviside unit step-function, $\theta(x)$ ionization threshold (I), energy parameter Δ and E_i. Δ is the factor that limits the effect of inelastic processes. In the original model of Staszewska *et al.* [34] have considered $\Delta=I$, which determines the threshold below which absorption is not allowed. However, this is not quite true since excitation can happen below the ionization threshold of the target as well. Hence, in the present case the original model is modified by considering Δ as an energy dependent parameter with first excitation energy of the target molecule as the lower limit [35,36]. This approximation is meaningful as it would allow the potential to penetrate more and allow electronic excitation channels to be included below ionization threshold of the target. Once all the model potentials are formulated, the radial part of the Schrödinger equation is solved by partial wave analysis using the Numerov method [37] for the given electron molecule system. The solution of the Schrödinger equation gives complex phase shift (δ_l) as its output, which carries the signature of electron target interaction for each partial wave. At low energies only few partial waves are required for convergence, but as the electron energy increases more and more partial waves would be required. These phase shifts are further employed to find the relevant cross sections [37] as,

$$Q_{inel}(E_i) = \frac{\pi}{k^2}\sum_{l=0}^{\infty}(2l+1)(1-\eta_l^2) \quad (7)$$

and

$$Q_{el}(E_i) = \frac{\pi}{k^2}\sum_{l=0}^{\infty}(2l+1)\left|\eta_l \exp(2i\,\mathrm{Re}\,\delta_l)-1\right|^2 \quad (8)$$

where $\eta_l = \exp(-2\,\mathrm{Im}\,\delta_l)$ is the inelasticity or absorption factor for each partial wave. The total cross section can then be easily obtained from the sum of equation (7) and (8).

3. Results and Discussion

The present calculation focuses on the electron impact total and elastic cross sections of disilane over a broad energy range from 0.1 eV to 5 keV. The electronic excitation and differential cross sections are also reported in the present study. The results obtained are presented in graphical form in Figs. 1-6. A comparison of resonance position and width predicted in the present calculation with existing data is given in table 2. The cross section data are tabulated in table 3. The data presented in this article is using SEP approximation, unless mentioned otherwise.

Table 2. Comparison of present resonance position and width of Si_2H_6 with the previous studies.

Symmetry	Present		Others
	Resonance Position (eV)	Resonance Width (eV)	Resonance Position (eV)
^{2}A'	3.37 (SE)	1.06 (SE)	2.5 [6]
	3.02 (SEP)	0.86 (SEP)	2.0 [12]
			3.4 [11] (SE)
^{2}A"	3.31 (SE)	1.06 (SE)	
	3.00 (SEP)	0.86 (SEP)	

Figure 1 shows the eigenphase diagram for the doublet scattering states (^{2}A' and ^{2}A") within the SEP approximation in the reduced point group symmetry (C_s) of the molecule. The study of eigenphase sum finds significance due to its capability in locating resonances appearing at low energy regime. These resonances appear as prominent structures in eigenphase sums (with change in it sign), vibrational excitation cross section and elastic cross section [38]. They can lead to dissociation of the molecule through electron attachment processes. From the eigenphase sum the position of the resonances can be identified by locating the energy at which the eigenphase sum goes through zero. In the present study, the calculations are carried out both within the SE and SEP approximation. The eigenphase diagram shows signature of resonances at 3.37 and 3.31 eV within the SE approximation and 3.02 and 3.00 eV within the SEP approximation for the ^{2}A' and ^{2}A" scattering states. This clearly indicates that inclusion of polarisation effect in the calculation shows the shifting of resonance position towards the low energy region. From table 2 it is evident that inclusion of polarization effects improves the calculation. Hence, inclusion of more correlation terms in the calculation may further improve the results. However, including all the correlation into the calculation is computationally taxing. Hence, in the present study the number of functions is restricted to obtain a reasonable result within an agreeable time frame. The resonances observed in the eigenphase sum can be clearly observed in the total cross section too, at the respective energies.

The present resonance position calculated within the SE approximation agrees quite well with the previous SE calculation of Bettega *et al* [11] using SMC method. The position of the resonance structure is shifted towards the left side as the polarization effects are included in the calculation at around 3 eV showing a reasonable agreement with Szmytkowski *et al* [6] at 2.5 eV and Dillon *et al* [12] at 2 eV. This confirms that the inclusion of polarization effect has improved the result in the present calculation.

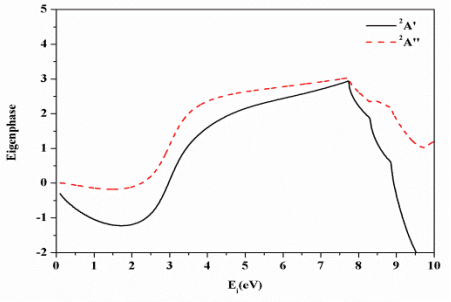

Fig. 1 Eigen phase sum for doublet scattering states of Si_2H_6.

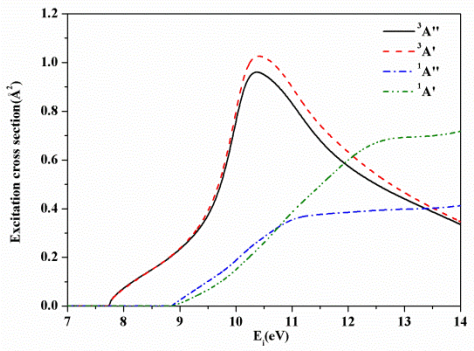

Fig. 2 Excitation cross sections for e-Si_2H_6 scattering.

The excitation cross sections for e-Si_2H_6 are plotted in figure 2 from the ground state to different singlet and triplet excited states (^{3}A", ^{3}A', ^{1}A" and ^{1}A'). The maximum contribution to the excitation cross section comes from the triplet excited states (^{3}A" and ^{3}A') and the threshold of the first excitation energy is at 7.74 eV for the ^{3}A" and ^{3}A' states. The threshold of the excitation energy for the singlet states (^{1}A" and ^{1}A') is around 9 eV. These cross sections show the probability of getting excited to various energy levels of the target. This is the first ever prediction of excitation cross section for the e-Si_2H_2 system to the best of our knowledge.

Table 3. Total cross section for e-Si_2H_6 scattering system.

E_i (eV)	Q-mol (Å^2)	E_i(eV)	SCOP (Å^2)
0.1	39.76	11	57.65
0.2	38.46	12	55.94
0.3	37.27	13	54.52
0.4	36.23	15	52.49
0.5	35.33	20	49.41
0.7	33.92	25	46.91
1	32.68	30	44.24
1.5	32.56	40	38.78
2	34.99	50	34.59
2.5	43.16	60	31.28
3	69.89	70	28.66
3.5	71.77	80	26.58
4	68.86	90	24.87
4.5	68.18	100	23.41
5	67.14	120	21.06
5.5	65.84	150	18.49
6	64.67	200	15.60
6.5	63.73	300	12.22
7	62.97	400	10.24
7.5	62.30	500	8.90
8	61.52	1000	5.60
8.5	60.67	2000	3.27
9	59.78	3000	2.34
9.5	58.65	4000	1.87
10	57.09	5000	1.57

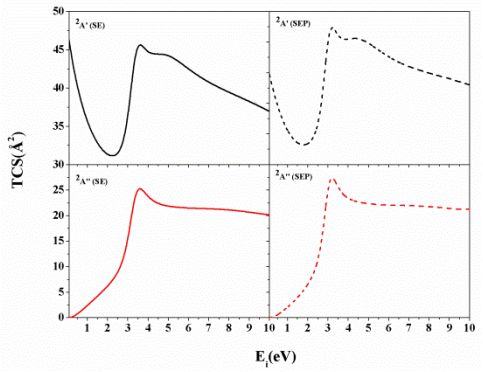

Fig. 3 Symmetry components of the total cross section for electron scattering by Si_2H_6.

Figure 3 shows the plot of total cross section for the symmetry components (^{2}A' and ^{2}A") of the C_s point group within the SE and SEP approximation used in the calculation. The maximum contribution to the total cross section comes from the ^{2}A' symmetry in both the models compared to ^{2}A" symmetry. The resonance position predicted by SE model for ^{2}A' and ^{2}A" symmetry is at around 3.3 eV. The inclusion for correlation polarization shifts the resonance position for both the symmetries from 3.3 to 3.0 eV.

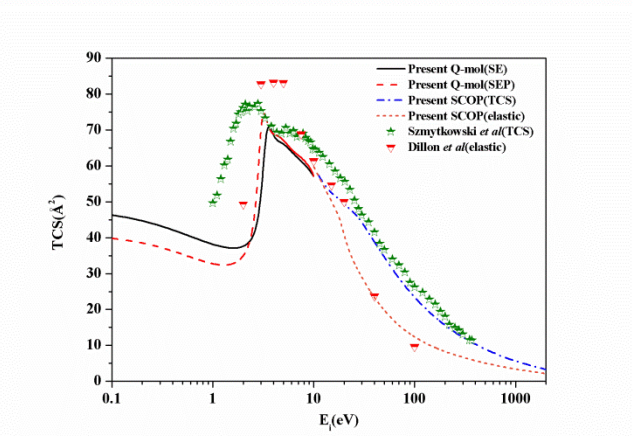

Fig. 4 Present cross sections (TCS and elastic) compared with the experimental results for e-Si_2H_6 scattering. Solid line: Present Q-mol (SE); Dash line: Present Qmol (SEP); Dash dot line: Present SCOP (TCS); Short dash line: Present SCOP (elastic); Star: Szymtkowski *et al* [6]; Triangle: Dillon *et al* [12].

For the sake of clarity and clear visibility of the cross section, the present TCS and elastic cross section (Q_{el}) is compared in two curves: one along with measurements and the other along with the calculations. Figure 4 shows the comparison of the present cross sections along with the experimental results of Szmytkowski *et al* [6] and Dillon *et al* [12]. The cross section of this molecule presents a shape resonance belonging to the two fold-degenerate ^{2}E symmetry of the D_{3d} group, which splits into the ^{2}A' and ^{2}A" symmetries of the C_s group. At low energies the present calculations predict resonances at 3.3 and 3.0 eV within the SE and SEP models respectively. The position of the resonance shows decent agreement with Szmytkowski *et al* [6] who observed the structure located at 2.5 eV. The integral elastic

cross section of Dillon *et al* [12] is slightly higher than Szmytkowski *et al* [6] and the present TCS data at the peak and they have observed broad maxima located at around 5 eV. However, Dillon *et al* [12] in their inelastic energy loss spectrum have observed the resonance to be located at 2 eV. The present SEP model has successfully predicted the resonance position at 3.0 eV which is quite close to experimental value of Dillon *et al* [12] and Szmytkowski *et al* [6] and shows a reasonable improvement from the previous SE calculations. After the threshold of the target the present Q_{el} data agrees quite well with the measurement of Dillon *et al* [12] till 100 eV.

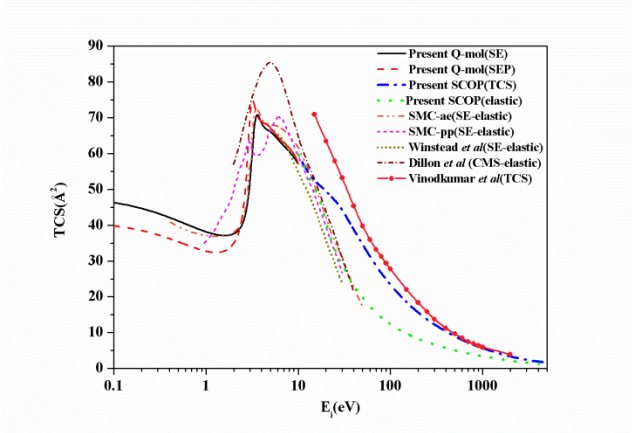

Fig. 5 Present cross sections (TCS and elastic) compared with the theoretical results for e-Si_2H_6 scattering. Solid line: Present Q-mol (SE); Dash line: Present Q-mol (SEP); Dash dot line: Present SCOP (TCS); Dot line: Present SCOP (elastic); Dash dot dot line: SMC–ae [11]; Short dash line: SMC-pp [9]; Short dot: Winstead *et al* [8]; Short dash dot line: Dillon *et al* [12]; Line+circle: Vinodkumar *et al* [14]

Figure 5 compares the present cross sections (TCS and elastic) with the available theoretical data of Winstead *et al* [8], Bettega *et al* [9,11], Dillon *et al* [12] and Vinodkumar *et al* [14]. At low energies the present SE calculation shows excellent agreement with the all electron Schwinger multichannel (SMC-ae) calculation of Bettega *et al* [11] done within the SE approximation throughout their energy range. The resonance structure predicted by both the calculations, present (SE) and the SMC-ae are very close to each other at 3.3 and 3.4 eV respectively. The pseudo-potential Schwinger multichannel (SMC-pp) calculation of Bettega *et al* [9] shows prominent structure around (2 - 3) eV and a weak structure around 7 eV. The SE elastic cross section calculation of Winstead *et al* [8] decreases monotonically with the increase of energy and shows a reasonable agreement with other results including the present one in terms of shape and nature of the cross section from 5 to 30 eV. The elastic cross section calculations of Dillon *et al* [12] by CMS method overestimates all other cross sections at the peak by some margin and predicts a broad resonance at around 5 eV. The present TCS computed within SEP approximation shifts the resonance structure from 3.3 to 3.0 eV which matches quite well with SMC-pp calculation of Bettega *et al* [9].

Below 50 eV the present result does not agree with Vinodkumar *et al* [14] which may be due to the difference in charge densities used in the calculation. Vinodkumar *et al* [14] have used Cox and Bonham [39] H-F parameters for the charge density, whereas in the present case the H-F parameters of Salvat *et al* [30] are used. It is interesting to note that the low energy R-matrix calculation and the intermediate energy SCOP cross section results gives very good matching at the overlap of two formalism at around the ionization potential of the target. This has helped to predict cross section over a wide energy range from 0.1 to 5000 eV using two distinct formalisms.

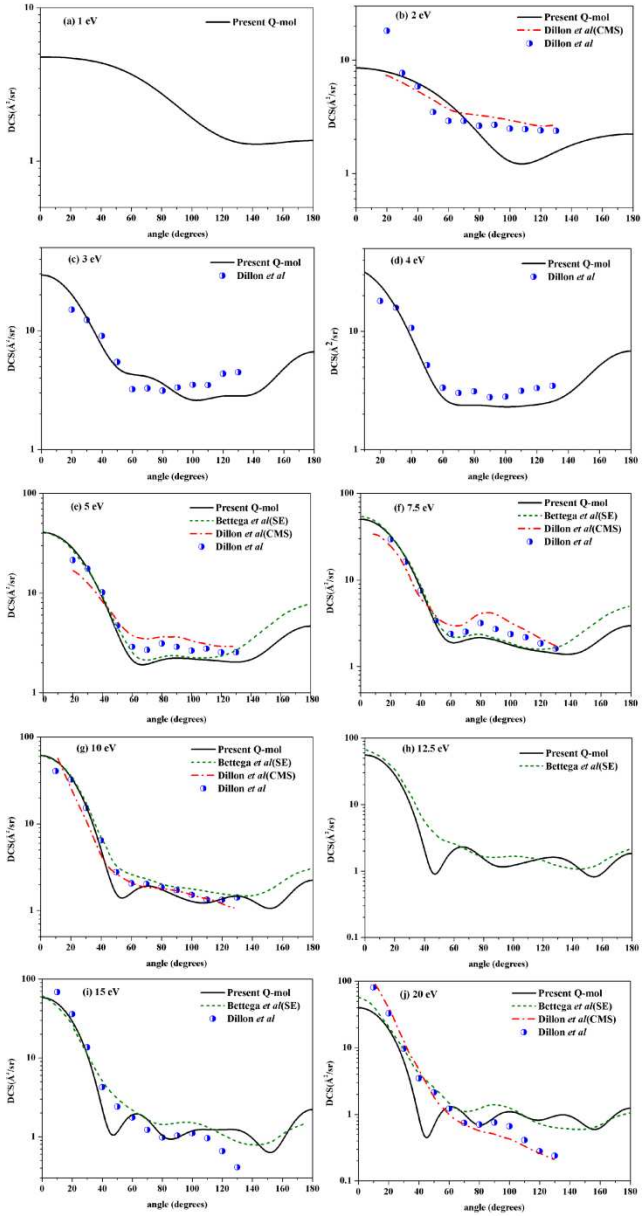

Fig. 6 Differential cross section (DCS) for e-Si_2H_6 scattering at different energies. Solid line: Present Q-mol; Short dash line: Bettega *et al* [10]. Dash dot line: Dillon *et al* (CMS) [12]; Circle: Dillon *et al* [12]

In figure 6 we have shown the differential cross section (DCS) for e-Si_2H_6 system at the energy range from 1 to 20 eV. The DCS was calculated within both SE and SEP models. However, only

SEP results are plotted along with the available comparison of Dillon *et al* [12] and Bettega *et al* [10]. Dillon *et al* have done the measurements of DCS at 2, 3, 4, 5, 7.5, 10, 20 eV and also computed the DCS for energies viz. 5, 7.5, 10 and 20 eV using CMS method. The experimental data shows reasonable agreement with CMS data for all the energies except at low angles from 20^0 to 50^0. The present DCS along with Bettega *et al* [10] shows excellent agreement at low angles, whereas agreement becomes reasonable at higher angles for 5, 7.5 10 and 20 eV with the experimental results of Dillon *et al* [12]. Bettega *et al* [10] have obtained oscillatory behavior in the DCS for the entire energy range which they attribute due to the coupling of higher angular momenta of the heavier inner atoms in the scattering process. The same oscillatory structures are also very much evident from the present calculations which get pronounced at higher energies. The inclusion of polarization effects in the calculations (SEP model) has improved the results at higher angles and a decent agreement is observed with the experiment [12] for energies 3, 4, 5, 7.5 and 10, 15 and 20 eV. It is worth noting here that as more states are included in the close coupling (CC) expansion and retained in the outer region calculation, DCS can give a much better agreement with the experiment showing an improved modeling of polarization interaction.

4. Conclusion

In the present study, the results of electron scattering with disilane molecule are presented. The results obtained are interpreted in terms of eigenphase sum and various cross sections such as excitation, total and differential. The methodology employed here is the R-matrix method for low energy regime (from 0.1 to 10 eV). Beyond 10 eV, the SCOP formalism was employed up to 5 keV. The target properties obtained for disilane by R-matrix method shows good agreement with other values found in the literature. This confirms the reliability of the target model employed for the calculation. The consistency of the results obtained by the two formalisms is quite good and shows a smooth transition at the overlapping energy (at around 10 eV). This has helped us to predict cross section over a wide energy range from 0.1 eV to 5 keV. The sudden variation in the eigenphase sums at around 3.3 and 3 eV within the SE and SEP models clearly indicates the presence of resonances during electron target interaction. This is very well reflected in the TCS at the same energies too. The structure present in the TCS at 3 eV within the SEP model shows a clear improvement over the previous calculations. Moreover, the positioning of the resonance shows a decent agreement with the experiments of Dillon *et al* [12] and Szmytkowski *et al* [6] whose resonances occur at 2 and 2.5 eV respectively. In general, the TCS obtained agrees well in terms of nature and shape of the curve with all the available experimental and theoretical cross sections. Intermediate to high energy calculations for total and elastic cross sections shows good agreement with the experiments of Szmytkowski *et al* [6] and Dillon *et al* [12]. The present elastic cross section also shows good agreement with other *ab-initio* calculations [8,9,11] from 10 eV to 30 eV. The excitation cross sections are computed for which there is no comparison available. These cross sections are important as it gives the probability of the target getting excited to different energy levels. The present DCS shows reasonable agreement with the experimental and theoretical data of Dillon *et al* [12] and Bettega *et al* [10] at low scattering angles. One of the motivations behind the present study was to the compare the results obtained with or without polarization effects in the calculation. It was found that the position of the resonance using the SEP model gave a better value than SE model in comparison with the experimental results. There is no straightforward way to calculate the uncertainty in the R-Matrix calculations. An alternate option is to repeat the calculation in several different ways like using different basis set, increasing the r-matrix radius or the size of CAS or the number of states included and estimate the sensitivity of the calculation to these changes. Even though the effect of these changes may be quite small, it is found that it improves the results. However, an increase in the r-matrix radius or the size of CAS or number of states included might be computational not viable. Hence, in the present case an optimized number is used without compromising the reliability of the results obtained. Moreover, this is the first ever study to find cross section for disilane over such a wide energy range (from 0.1 eV to 5 keV). The present results can be very useful for modeling various plasma environments containing disilane molecule.

Acknowledgements

BA thanks Department of Science and Technology, New Delhi for financial support through Research Project Grant SR/S2/LOP-11/2013, under which part of this work is carried out.

Notes and references

Department of Applied Physics, Indian School of Mines, Dhanbad, 826004, Jharkhand, India. Tel: +91 9470194795; E-mail: bka.ism@gmail.com

1. S. D. Brotherton, C. Glasse, C. Glaister, *et al.*, *Appl. Phys. Lett.* 2004, **84**, 293.
2. H. Sukti and R. Swati, *Solid State Commun.* 1998, **109**, 125.
3. J. Ihm and J. D. Joannopoulos, *Phys. Rev. B*, 1981, **24**, 4191.
4. M. J. Kushner, *J. Appl. Phys.* 1988, **63**, 2532.
5. J. Hanna, T. Ohuchi and M. Yamamoto, *J. Non-cryst. Solids*, 1996, **198-200**, 879.
6. C. Szmytkowski, P. Mozejko and G. Kasperski, *J. Phys. B: At. Mol. Opt. Phys.* 2001, **34**, 605.
7. X. H. Wan, J. H. Moore and J. A. Tossel, J. Chem. Phys. 1989, **91**, 7340.
8. C. Winstead, P. G. Hipes, M. A. P. Lima and V. Mckoy, *J. Chem. Phys.* 1991, **94**, 5455.
9. M. H. F. Bettega, L. G. Ferreira and M. A. P. Lima, *Phys. Rev. A*, 1993, **47**, 2.
10. M. H. F. Bettega, A. J. S. Oliveira, A. P. P. Natalense, M. A. P. Lima and L. G. Ferreira, *Eur. Phys. J. D.* 1998, **1**, 291.
11. M. H. F. Bettega, C. Winstead and V. Mckoy, *J. Chem. Phys.* 2003, **119**, 2.
12. M. A. Dillon, L. Boesten, H. Tanaka, M. Kimura and H. Sato, *J. Phys. B: At. Mol. Opt. Phys.* 1994, **27**, 1209.
13. M. A. Dillon, D. Spence, L. Boesten and H. Tanaka, *J. Chem. Phys.* 1988, **88**, 4320.
14. M. Vinodkumar, C. Limbachiya, K. Karot and K. N. Joshipura, *Eur. Phys. J. D*. 2008, **48**, 333.

15. J. Tennyson, *Phys. Rep.*, 2010, **491,** 29.
16. A. Jain and K. L. Baluja, *Phys. Rev. A*, 1992, **45**, 202.
17. B. Goswami, R. Naghma and B. Antony, *Phys. Rev. A*, 2013, **88**, 032707.
18. A. Barot, D. Gupta, M. Vinodkumar and B. Antony, *Phys. Rev. A*, 2013, **87**, 062701.
19. D. Gupta and B. Antony, *J. Electron Spectrosc. Relat. Phenom.* 2013, **186**, 25.
20. Website: http://cccbdb.nist.gov/
21. K. Takatsuka, V. McKoy, *Phys. Rev. A*, 1981, **24**, 2473.
22. B. I. Schneider, T. N. Rescigno, *Phys. Rev. A*, 1988, **37,** 3749.
23. S. N. Altunata, S. L. Coy and R. W. Field, *J. Chem. Phys.* 2005, **123**, 084318.
24. S. N. Altunata, S. L. Coy and R. W. Field, *J. Chem. Phys.* 2005, **123**, 084319.
25. B. M. Wong, S. N. Altunata and R. W. Field, *J. Chem. Phys.* 2006, **124**, 014106.
26. A. M. Arthurs and A. Dalgarno, *Proc. Phys. Soc., London, Sect. A*, 1960, **256,** 540.
27. A. Faure, J. D. Gorfinkiel, L. A. Morgan, and J. Tennyson, *Comput. Phys. Commun.* 2002, **144**, 224.
28. M. Gailitis, *J. Phys. B*, 1976, **9**, 843.
29. N. Sanna and F. A. Gianturco, *Comput. Phys. Commun.* 1998, **114**, 142.
30. F. Salvat, J. D. Martinez, R. Mayol and J. Parellada, *Phys. Rev. A*, 1987, **36**, 467.
31. Gradashteyn and I. M. Ryzhik, Tables of Integrals, Series and Products (Associated Press, New York, (1980).
32. S. Hara, *J. Phys. Soc. Japan*, 1967, **22,** 710.
33. X. Zhang, J. Sun, and Y. Liu, *J. Phys. B: At. Mol. Opt. Phys.*, 1992, **25,** 1893.
34. G. Staszewska, D. W. Schwenke, D. Thirumalai, and D. G. Truhlar, *Phys. Rev. A*, 1983, **28,** 2740.
35. B. Goswami, R. Naghma and B. Antony, *Mol. Phys.*, 2013, **111**, 3047.
36. M. Vinodkumar, C. Limbachiya, B. K. Antony and K. N. Joshipura, *J. Phys. B: At. Mol. Opt. phys.* 2007, **40**, 3259.
37. C. J. Joachain, in Quantum Collision Theory (Amsterdam: North-Holland, 1983).
38. L. Andric, I. M. Cadez, R. I. Hall and M. Zubeck. *J. Phys. B*, 1983, **16,** 1837.
39. H. L. Cox and R. A. Bonham, J. *Chem. Phys.*, 1967, **47,** 2599.